sustainability

MDPI

*Article*

# Geomechanical Characterization of Unwelded Volcanic Bimrock Materials for Sustainable Slopes: Application to Road Instability Problems in the Western Cordillera of Ecuador

**Marlon Ponce-Zambrano [1,*], Julio Garzón-Roca [2], Francisco J. Torrijo [3] and Olegario Alonso-Pandavenes [1]**

1 Facultad de Ingeniería en Geología, Minas, Petróleos y Ambiental (FIGEMPA), Universidad Central del Ecuador, Quito 175000, Ecuador; omalonso@uce.edu.ec
2 Department of Geodynamics, Stratigraphy and Paleontology (GEODESPAL), Faculty of Geology, Complutense University of Madrid, 28040 Madrid, Spain; julgarzo@ucm.es
3 Department of Transport and Geotechnical Engineering, Research Centre PEGASO, Universitat Politècnica de València, Camino de Vera S/N, 46022 Valencia, Spain; fratorec@trr.upv.es
* Correspondence: mrponce@uce.edu.ec

**Abstract**

This paper presents a geomechanical characterization for unwelded volcanic bimrock materials. Bimrocks are geological materials consisting of blocks of rock of different sizes embedded in a finer matrix. Many volcanic deposits and outcrops can be classified as bimrocks, and some of them correspond to unwelded bimrocks, i.e., with the absence of strong bonds between blocks of rock and matrix. The geomechanical characterization proposed is oriented towards bimrocks slopes, their stability and landslide hazard occurrence. It consists of five steps which includes the material description, the volcanic deposit classification, the definition of block size range, the computation of the volumetric block percentage, the geotechnical characterization of the blocks of rock, and the geological and geotechnical analysis of the matrix that surrounds the blocks. The geomechanical characterization proposed is applied to four slopes at the Western Cordillera of Ecuador, where slopes instabilities are common. Results show that the geomechanical characterization sets a reliable framework for geotechnically describing bimrocks materials, explaining the actual stability state of the slopes. It also enables taking appropriate and optimum decisions in the design and management of volcanic slopes, thus contributing to a sustainable approach of landslide mitigation.

**Keywords:** geomechanical characterization; bimrock; volcanic deposit; landslides; Western Cordillera of Ecuador; sustainability



Academic Editor: Kaihui Li

Received: 10 June 2025
Revised: 26 July 2025
Accepted: 1 August 2025
Published: 5 August 2025

**Citation:** Ponce-Zambrano, M.; Garzón-Roca, J.; Torrijo, F.J.; Alonso-Pandavenes, O. Geomechanical Characterization of Unwelded Volcanic Bimrock Materials for Sustainable Slopes: Application to Road Instability Problems in the Western Cordillera of Ecuador. *Sustainability* **2025**, *17*, 7080. https://doi.org/10.3390/su17157080



## 1. Introduction

Volcanic geological materials are responsible of many landslides and rockfalls. Their high recurrence in steep areas, such as in the Andes, is a constant problem affecting infrastructures and urban areas, with a major impact on public safety. Many of these mass movements involve mixtures of heterogeneous volcanic rocks particles of different grain sizes and scales. Such mixtures rock mélanges are known as “bimrocks”, a short form of “Block in matrix rocks” [1,2]. They are defined as mixtures of blocks of rock within a finer-textured matrix. In terms of strength, the blocks of rock hold higher geotechnical strength parameters than the matrix grain. The heterogeneity, randomness, and uncertainty of volcanic geomaterials raise questions about how to approach the characterization and parameterization of these heterogeneous materials from a geological and geotechnical engineering perspective [3].

Bimrocks are characterized by [2,4]: (i) a mechanical strength contrast, where the blocks of rock have higher strength than the matrix that surrounds them; (ii) a size range of the blocks of rock; and, (iii) a volumetric block percentage (VBP), defined as the relation, in percentage, between the area of blocks of rock and the matrix area, for a total area of 1 $m^2$. The Literature has shown [5–7] that there is a good relationship between the VBP and the mechanical behavior of a bimrock. Such mechanical behavior is independent of the size of the blocks in relation to the scale of the problem, and there is also no dependence on the overall structure orientation of the blocks of rock.

Sampling has been shown to be a problem when studying bimrocks. Some attempts were conducted to overcome this difficulty and obtain geotechnical parameters (e.g., cohesion, friction angle, static and dynamic moduli) in laboratory studies [8–10]. Other techniques refer to the use of qualitative and quantitative characterization by stochastic methodologies. For instance, Wen-Jie et al. [11] used image processing for computing VBP, and their results were used for building large-scale samples for in situ direct shear tests.

An exponential correlation between the uniaxial compressive strength (UCS) and VBP has been recognized. Some authors [9,12,13] used empirical models based on reconstituted specimens of matrix mixtures with pieces of rocks. From that they developed an empirical strength zoning based on core samples, applying Mohr-Coulomb and Hoek-Brown failure models. Kalender et al. [10] proposed predicting the strength in non-welded bimrocks through artificial specimens. Coli et al. [14] tested in situ bimrocks and established that the higher the VBP, the higher the frictional strength and the lower the cohesion.

Two main types of volcanic bimrock materials are found: welded (e.g., agglomerate) and unwelded (e.g., loose pyroclastic flows). The later are the aim of this work. In this regard, the literature [8,13,15] shows the difficulty of both sampling and obtaining core samples in unwelded bimrock materials.

Jiménez-Rodríguez [16] identified the difficulty of understanding the stochastic nature of volcanic deposits and their block geometry in relation to the matrix, and they proposed the use of probability theory [17,18]. Sonmez et al. [19] used block count and VBP to obtain UCS and deformation moduli in volcanic bimrocks, applying 1D and 2D fractal (random/probabilistic) techniques and developing prediction models using regression analyses. Results showed that the UCS of agglomerate cores decreases as block count increases. A similar result was obtained for the elastic moduli of the agglomerate cores.

Nikolaidis and Saroglou [20] proposed to improve field evaluation when studying bimrocks. They proposed to include the following: (i) a documentary study and field investigation; (ii) walk-through study and site(s) selection; (iii) choice of an appropriate project scale; (iv) acquisition of exploration lines for linear block proportions of the studied outcrops; (v) geological description according to a list of proposed parameters; (vi) image analysis for stereological analysis (to obtain VBP and block size distribution); (vii) classification and characterization of the matrix and the blocks of rock.

Wang et al. [21] performed dynamic tests on bimrocks and established that the content of the blocks of rock and the confining pressure influence the dynamic characteristics of the bimrock. Napoli et al. [22–24] studied tectonic and sedimentary heterogeneous geological units composed of bimrocks. They confirmed that the mechanical behavior of these formations depends on the percentage of VBP [6,9,13,25], but there are probably other factors that also influence their mechanical behavior; in particular, finite element modeling was used to investigate the influence of the shape and orientation of the blocks of rock on the slope.

Although the number of research works on bimrocks has been increasing, a clear methodology to address the geomechanical characterization of a bimrock is absent, especially on bimrock materials of volcanic nature. In this context, this work proposes a geomechanical characterization for unwelded volcanic bimrocks to be easily applied by researches and practitioners. The geomechanical characterization comprises five steps (Figure 1): (i) material description and volcanic deposit classification; (ii) characteristic dimension and block size range definition; (iii) VBP computation; (iv) rock blocks characterization; and (v) matrix analyses. As a novelty, the first step of the geomechanical characterization focuses on understanding the nature of the volcanic deposit and if they correspond to initial volcanic emission phases or transport stages, thus differentiating three deposit types: debris avalanches, pyroclastic flows and lahars. In addition, apart from considering rock and matrix strength parameters, the geomechanical characterization proposed also considers the chemical and mineralogical composition (via XRF and XRD analyses) and grain size distribution of the matrix to achieve a better understanding of the mechanical behavior of volcanic bimrocks. The present study also proposes a systematic and accessible method based on image analysis and the use of meshes combined with stereological techniques to estimate VBP. All in all, the methodological approach proposed integrates multidisciplinary concepts, including soil and rock mechanics, mineralogical characterization, and geotechnical testing, as addressed by various authors [1–21].

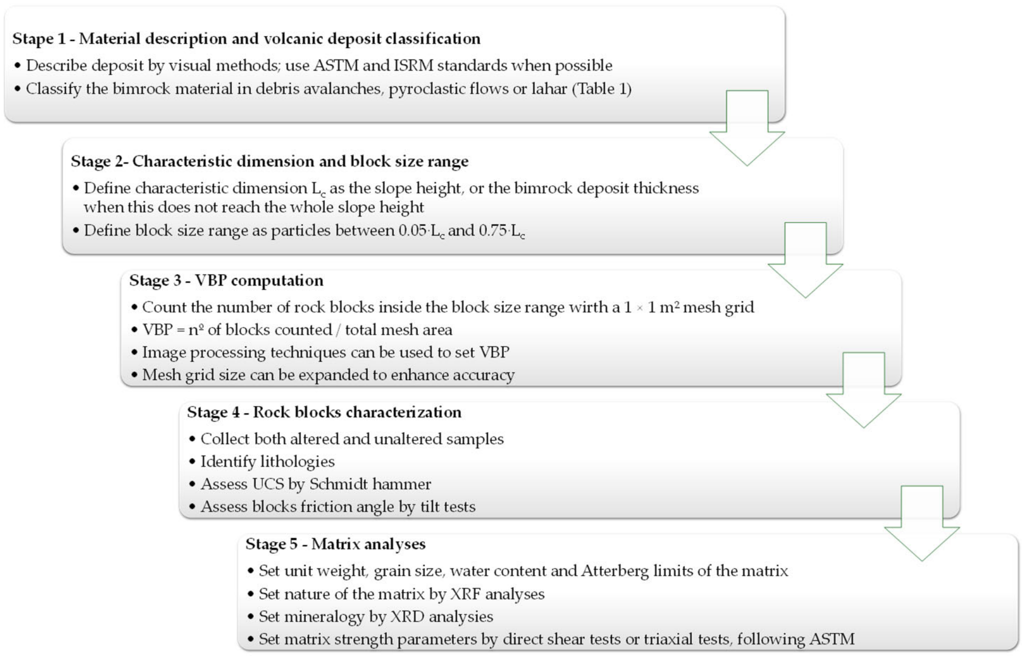


**Figure 1.** Geomechanical characterization proposed for unwelded volcanic bimrocks flow chart.

The geomechanical characterization proposed is applied to four road slopes of the Western Cordillera of Ecuador. Landslides occurrence in Ecuador is a common social and economic problem [26–30] and volcanic bimrock materials can frequently be found in the Western Cordillera [31]. Application of the geomechanical characterization proposed results in a systematic collection of data. The subsequent analyses based on that show the usefulness of the geomechanical characterization, as a first stage, to understand the mechanical behavior of the slopes studied as well as its stability.

Thus, the geomechanical characterization proposed contributes to the knowledge of unwelded volcanic bimrocks. In addition, it may help in the assessment of nature and anthropic slopes, as well as in the design of the corresponding stabilization measures. Moreover, it contributes to the sustainable management of landslides, by fostering strategies and procedures that reduce the social impact of such hazards in an environmentally responsible and economically viable way [30,32,33]. The balance between hazard mitigation and resource preservation is one of the pillars of the Sustainable Development Goals [34]. Taking appropriate and optimum decisions in the design and management of volcanic slopes that can affect infrastructure, villages, and urban areas is essential to avoid significant recurring economic costs [16], and this also helps in the protection of natural cultural heritage and encourages its sustainable conservation and fruition [35–37].

## 2. Geomechanical Characterization Proposed for Unwelded Volcanic Bimrocks Slopes

### 2.1. Material Description and Volcanic Deposit Classification

The first step for geomechanically characterizing an unwelded volcanic bimrock outcrop is conducting a proper geological description. This description should be performed including deposit thickness, terrain morphology, texture, structure, composition, grain size and sorting (visual), color, lithology, degree of consolidation, and presence of hydrothermal alteration, and it should be based on common standards like ASTM D2488 [38].

From such a description, this work proposed to classify the unwelded volcanic bimrock deposits [39,40] into three types: debris avalanches, pyroclastic flows, and lahars. Table 1 shows the geomorphological, structural and compositional criteria that define each deposit type and enables its identification by a practitioner. It should be noted that pyroclastic surges, block and ash flows and similar deposits are not considered in this classification since either their maximum grain size is small and the big particles cannot be considered as blocks of rock, or matrix and rock blocks are welded.

**Table 1.** Deposit classification for unwelded volcanic bimrocks; based on the work of [39,40].

| | Debris Avalanche | Pyroclastic Flows | Lahar |
|---|---|---|---|
| Morphology | Irregular deposit dominated by the presence of hummocks and scars; result of volcanic edifices collapse, associated or not with eruptions; heterogeneous and heterometric blocks transported without completely disintegrating during movement | Pyroclastic fragments; blocks, bombs, lapilli, ash; identification of the sequence of deposits and their relationship to each other; layered structures | Subhorizontal morphology; dense flow of fragments and water. |
| Texture | Poorly sorted deposits; wide grain size distribution; presence of metric blocks | Granulometry, shape and degree of organization of the fragments; decreasing or inverse degree | Angular blocks in a sand-silt-clay matrix |
| Structure | Fractured blocks retain interlocking fitting; presence of jigsaw-fits and/or jigsaw-cracks; intrablock destruction structures sub coherent fracturing during transport, without total loss of its original morphology | Layers, lenses and contacts; agglomerates, consisting mainly of blocks, volcanic breccias; ignimbrites | Chaotic, mixture of materials |
| Composition | Multiple lithologies found; dacite fragments if coming from dome, and andesites, basalts and sedimentary lithics if coming from the volcano base | Varied; one lithology dominates | Composed of water, ash and rock fragments of various sizes and lithologies |
| Other | Blocks scattered on the surface or buried within the body of the avalanche; low mobility; chaotic matrix; large blocks | Stratigraphic sequence; porosity low mobility; large blocks not common | High mobility; high water common; small blocks dominate, but may include boulders up to 30 cm or more |

### *2.2. Characteristic Dimension and Block Size Range*

The second step is establishing a criterion for differentiating the blocks of rock from the matrix. A "block of rock" in a bimrock is not a particle dimension itself, but a large particle with higher resistance than the matrix. A characteristic dimension ($L_c$) is defined [2,4,5]; this value is related to the scale of engineering interest for the problem under consideration. For the case of a slope, the value of $L_c$ is normally considered equal to the slope height [2]. If the geological structure of the slope consists of different layers and the bimrock deposit does not reach the whole slope height, $L_c$ may be taken equal to the bimrock deposit thickness; particularly, this approach should be followed if the slope height is much larger than the deposit thickness.

Once $L_c$ is computed, particles that can be considered blocks of rock are found in the range ($0.05 \cdot L_c$, $0.75 \cdot L_c$) [5]. Particles smaller than $0.05 \cdot L_c$ are part of the matrix; particles in the given range (hereafter named as "block size range") are blocks of rock; finally, particles bigger than $0.75 \cdot L_c$ should be considered as a rock mass and/or an independent element that does not belong to the bimrock.

### *2.3. VBP Computation*

The third step is computing the volumetric block percentage (VBP), i.e., the relation, in percentage, between the area of blocks of rock (particles inside the block size range) and the matrix area, for a total area of 1 $m^2$ [2,4].

Although the literature contains different techniques for computing the VBP, this work proposes (Figure 2) using a manual block count performed by a mesh grid with a scale of $1 \times 1$ $m^2$, following the method of Ettinger et al. [41]. This approach allows for the estimation of the VBP by measuring block diameters relative to matrix diameters, thereby defining the corresponding block and matrix volume percentages. It is interesting to note that this broader scale offers a more comprehensive assessment of the block proportion in the field, in contrast to the linear scanline method proposed by Nikolaidis and Saroglou [20]. In addition, the selected technique is much simpler to apply in the field than fractal techniques [19], and by collecting graphic data of the outcrop, including frontal and lateral photographs, image processing techniques [11] can be used to easily and accurately compute the VBP.

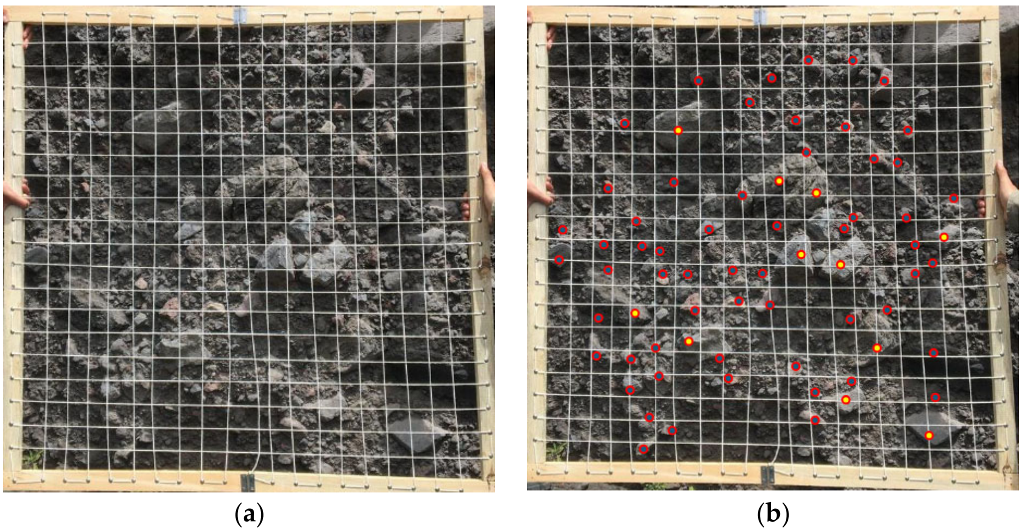

**Figure 2.** Block count for the determination of VBP, taking into account the scale effect: (**a**) 1 m × 1 m mesh; (**b**) block count of those particles inside the block size range defined by the interval ($0.05 \cdot L_c$, $0.75 \cdot L_c$).

To improve the representativeness of the outcrop and enhance the accuracy of the scale-dependent analysis, the mesh can be expanded to a 2 × 2 $m^2$ grid or even more. Having a greater mesh size may improve the representativeness of the estimation of VBP when blocks of rock are of high dimension, as is the case with debris flows. However, in oth-er volcanic deposits, like pyroclastic flows, a mesh size of great dimension may lead to a poor estimation of VBP due to the existence of small blocks of rock, thin layers and/or the natural high heterogeneity of such deposits. In volcanic outcrops with very small or very large blocks, the choice of mesh size must balance statistical representativeness with prac-tical feasibility.

Once the VBP is obtained, it should be checked that this value is equal to or greater than 25%, otherwise the material should be considered, in mechanical terms, a soil instead of a bimrock [6].

### 2.4. Rock Blocks Characterization

The fourth step consists of characterizing the blocks of rock. It is advisable to collect both altered and unaltered samples from the blocks of rock. From them, their lithology should be identified. This can be performed by visual methods, with the help of a magnifying glass. On each block, uniaxial compression strength (UCS) can be assessed using the Schmidt hammer. Similarly, the blocks friction angle can be determined by a tilt test. Other parameters to measure include the unit weight and the weathering grade of the blocks samples. All these tests should be performed according to the ISRM recommendations [42].

### 2.5. Matrix Analyses

The fifth and last step deals with the characterization of the matrix. One basic parameter here is the unit weight. When undisturbed samples from the matrix are obtained, unit weight can be found at the laboratory by the paraffin method, following ASTM D7263 [43]. Otherwise, unit weight can be determined in situ by a volumetric procedure, such as that used in ASTM D1556 [44]. Water content, gradation curve, and Atterberg limits can be obtained from any disturbed sample following ASTM D2216 [45], ASTM D422 [46] and ASTM4318 [47], respectively. In addition, the Unified Soil Classification System (USCS) [48] should be used to geotechnically classify the matrix. If an undisturbed sample from the matrix is possible to be obtained, a strength test should be performed, either direct shear tests or triaxial tests, following ASTM D3080 [49] and ASTM D4767 [50], respectively.

To determine the nature of the matrix, an X-ray fluorescence (XRF) analysis may be conducted, and the chemical composition obtained can be used to classify the volcanic rock by the Total Alkali Silica (TAS) diagram. XFR should be performed when there is any suspicion that the matrix and blocks of rock might not have the same lithological origin. In addition, having information about the nature of the matrix may be of interest in volcanic bimrocks since those materials undergo a high degree of fragmentation and fracturing during transport and deposition processes, which leads to increasing the exposure of the matrix to weathering agents and to accelerating potential mineralogical alteration (especially in tropical regions where high humidity and temperature intensify chemical weathering processes). XRF allows the detection of mineral phases susceptible to dissolution in the presence of water, which is particularly important in unconsolidated granular materials. Similarly, an X-ray diffraction (XRD) analysis may be conducted to determine the mineralogy of fines and quantify clay content, thus complementing the basic identification tests performed previously. Thus, conducting an XRD analysis is advisable when the intense weathering of rock block lithology may result in yielding a great amount of clay minerals that leading to a clayey behavior of the matrix. Clay minerals introduce a cohesive behavior between the blocks and the matrix particles. In addition, since clay is non-permeable, pore overpressures may be generated in the bimrock deposit during raining periods. However, XRF and XRD laboratory tests may be considered not mandatory in the geomechanical characterization proposed, especially since both analyses are expensive.

## 3. Application to the Ecuadorian Andes

### 3.1. Background and Vases Studies Selected

Ecuador, located in the northwest of South America, is characterized by its most prominent physiographic feature, the Andes (Figure 3). The western segment of the Andes divides Ecuador longitudinally into three distinct zones: the coastal plain to the west, the mountainous region in the center, and the eastern plain. Volcanic materials are mainly found in the mountainous region and cause many slope instabilities.


**Figure 3.** Geographical location of Ecuador and the Western Cordillera.

Volcanic lithologies in the Western Cordillera of Ecuador include volcanic avalanches, pyroclastic flows and lahars, all of which display characteristics of bimrock structures. Such bimrocks are exposed along several important road corridors, including the "Alóag–Tandapi–Santo Domingo", "Baños–Penipe–Patate", "Riobamba", and "Mitad del Mundo–Calacalí–Nanegalito" roads [31]. The E-20 highway, i.e., the "Alóag–Tandapi–Santo

Domingo" road, is the most important roadway constructed between the Western Andes of Ecuador and the coastal region; it extends over 98.7 km (Figure 4). Many instabilities were recorded throughout the years due to bimrock materials along the E-20 highway. Table 2 shows the frequency of landslides and rockfalls from 2012 to 2023, as well as the triggering factors and casualties. In 11 years, 39 landslides/rockfalls were recorded, affecting many sections of the road and causing 15 casualties. In addition, 549 traffic accidents occurred due to the instabilities. As an example, Figure 3 shows the state of the E-20 highway at kilometric point 83 (K83) in November 2023 after a rockfall. Data reveals that many instabilities were triggered by intense rainfalls, which is commonly considered the greatest frequency source of landslides/rockfalls in mid-elevation mountain areas with high rainfall events [51]. In Ecuador, however, earthquakes and erosion also play an important role in inducing instabilities.


(**a**) (**b**)

**Figure 4.** Rockfalls/landslides affecting K83 E-20 road in November 2023: (**a**) Shallow flat failure with blocks at mid-slope in the orientation of the slope, welded blocks larger than 3 m, and unwelded block with a matrix of less than 0.4 m. (**b**) Large size material, blocks larger than 3 m and fine matrix conglomerates.

**Table 2.** Landslide/rockfall frequency in the "Aloag–Tandapi -Santo Domingo" road, 2012–2023.

| Year | Month | Location (K. Point) | Instability | | Trigger Factor [2] | Casualties |
|---|---|---|---|---|---|---|
| | | | No. | Type [1] | | |
| 2012 | Mar | 40–70 | 12 | RF | EQ; RF; ER | 0 |
| 2013 | Feb; Apr; May | 40–70 | 1 | LD | EQ; RF; ER | 0 |
| 2014 | Mar; Apr | 28 | 2 | LD | RF | 0 |
| 2015 | Apr | 28 | 2 | LD | RF | 11 |
| 2016 | Jan; Apr; May | 34 | 3 | RF and LD | RF | 0 |
| 2017 | Apr; May; Jun | 48; 56; 63 | 3 | RF and LD | RF | 0 |
| 2018–2019 | Jan; Feb; Nov; Dec | 48–57 | 4 | RF | EQ; RF; ER | 2 |
| 2020 | Jan; Jun | 54 | 2 | RF | EQ; RF; ER | 0 |
| 2021 | Mar; Apr | 45 | 2 | LD | RF | 0 |
| 2022 | Feb; Apr; May | 27; 30; 79 | 3 | RF | RF | 0 |
| 2023 | Mar; Apr; Nov | 32; 43; 51; 83 | 5 | RF and LD | RF | 2 |

[1] RF: rockfall; LD: landslide. [2] EQ: earthquake; RF: intense rainfall and ER: erosion.

Studies on landslides cause by volcanic deposits in Ecuador are scarce, and the few that exist do not focus on it. For instance, the Development and Management Territorial Plan of Manuel Cornejo Astorga-Tandapi Parish [52] identifies that only 5% of the damage may be caused by susceptibility to mass movements, minimizing one of the most recurrent problems. Similarly, although some actions were conducted on the E-20 highway to address the instability problems, the absence of reference data for characterizing bimrocks led to barely solving it; as Table 2 shows, slope instabilities have been occurring continuously throughout the years.

The diversity of geological materials in the eastern sector of the Western Cordillera of Ecuador includes sources of ancient deposits dating from the Late Cretaceous to the Oligocene [53]. Over them, Neogene and Quaternary volcanic materials currently observed were sequentially deposited (Figure 5a). These deposits are situated along the flanks and slopes of major volcanic cones, whose edifices and materials were emplaced primarily toward the west (Figure 5b). The study area is delimited: in its northern part by the Atacazo-Ninaguilpa volcanic complex, whose deposits date from 222 ka to 71 ka [54]; in its southern part by the Corazón Volcano, whose deposits date from 115 ka to 70 ka [55].

In this context, the proposed geomechanical characterization was applied to four slopes (Figure 6) with exposed volcanic bimrock deposits found in the Western Cordillera of Ecuador:

- S-PB1, "Penipe-Baños" road at K32.
- S-PB2, "Penipe-Baños" road at K4.
- S-E490, "Riobamba" E-490 road at K7.
- S-E20, "Aloag–Tandapi" E-20 road at K34

### *3.2. Geomechanical Characterization of the Slopes Studied*

Table 3 summarizes the results of the application of the geomechanical characterization proposed across the four slopes studied. The type of deposit was defined following the classification given in Table 1. Material description, as well as rock and soil tests, were carried out according to ASTM and ISRM standards. Engineering dimension $L_c$ was defined as the thickness of the bimrock outcrop (deposit), and from this value, the block size range was computed. The VBP was obtained by a mesh grid with a scale of $1 \times 1$ m$^2$. All matrix analyses were conducted at the Laboratory of FIGEMPA at the Universidad Central del Ecuador.

**Table 3.** Geomechanical characterization proposed applied to the four slopes of the Western Cordillera of Ecuador (XFR, XRD and other matrix analyses are omitted).

| Slope | S-PB1 | S-PB2 | S-E490 | S-E20 |
|---|---|---|---|---|
| Total height (m) | 17 | 35 | 8 | 47 |
| Slope angle (°) | 70 | 65 | 70 | 70 |
| Bimrock deposit thickness (m) | 17 | 3 | 7 | 17 |
| Volcanic deposit | Debris avalanche | Pyroclastic flow | Debris avalanche | Debris avalanche |
| Description | Jigsaw crack, 2 facies, andesite and andesites with vesiculates, blocks > 20 cm | Rounded blocks from pyroclastic flows and the incorporation of clasts from other series. | Diameter of clasts 16 cm in the larger rock and 0.5 cm in the smaller rock | Andesite rock clasts, silty sandy matrix, size less than 0.1 cm–500 cm |
| $L_c$ (cm) | 17 | 3 | 7 | 17 |
| Block size range (cm) | 0.85–12.75 | 0.15–2.25 | 0.35–5.25 | 0.85–12.75 |
| VBP (%) | 85 | 27 | 55 | 75 |
| Block rocks UCS (MPa) | 93 | 57 | 45 | 87 |
| Block rocks friction angle (°) | 31 | 48 | 35 | 35 |
| Block rocks unit weight (kN/m$^3$) | 21.3 | 21.7 | 20.2 | 22.7 |
| Matrix unit weight (kN/m$^3$) | 20.7 | 27.8 | 24.2 | 19.4 |

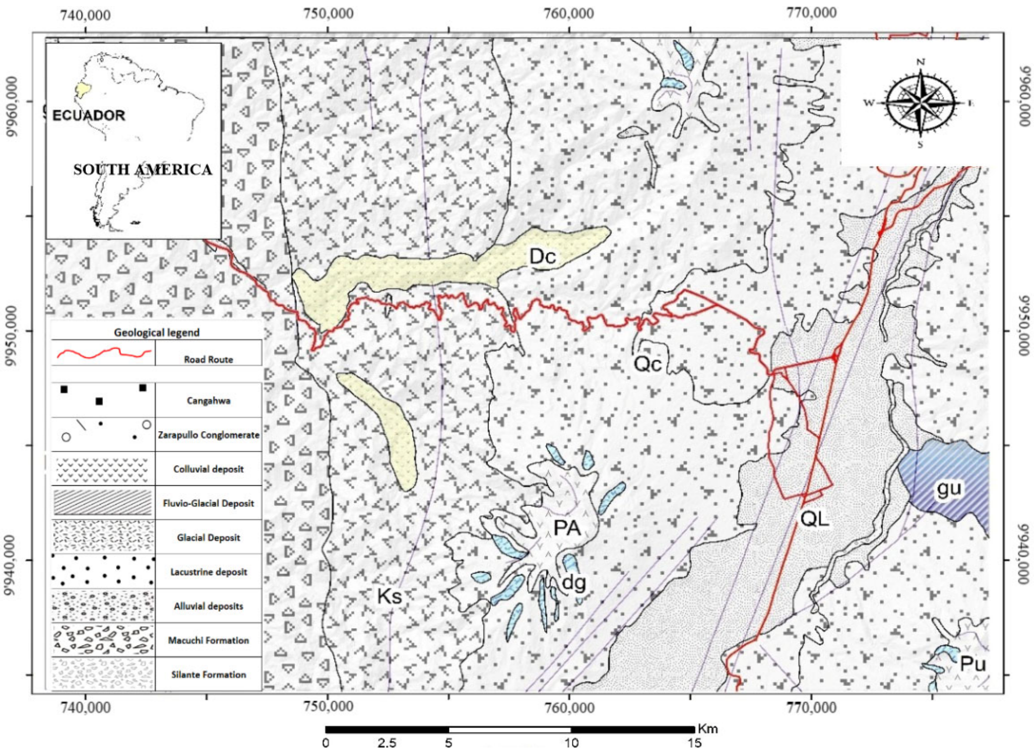


(**a**)

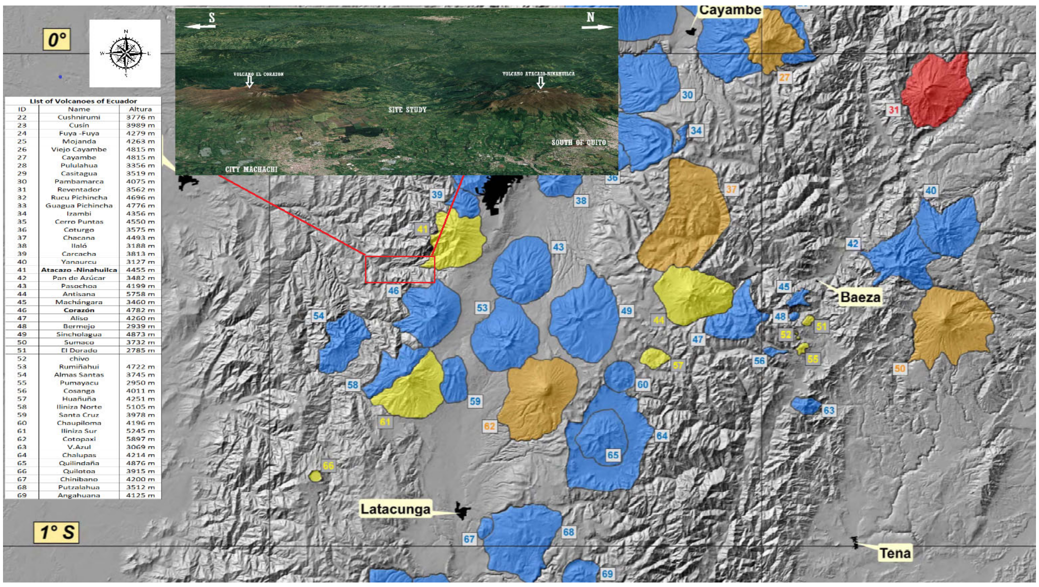


(**b**)

**Figure 5.** Geological and geomorphological setting of the area under study: (**a**) Local geologic map, modified from the study of [56]; (**b**) Scheme of the Quaternary volcanism of Ecuador around the study area, modified from the study of [57].

All slopes had an inclination equal to or greater than 65°. Slope S-PB1 had a total height of 17 m, and the whole slope was formed by a volcanic bimrock deposit. The outcrop corresponded to a typical structure of clasts and debris avalanche, where the clasts produced by their transport are fractured and angular. Jigsaw crack structures, typical of avalanches, were observed. The deposit presented several levels of color, with chaotic, heterogeneous, and heterometric blocks, also with different directions of their arrangement. Thus, this slope was classified as debris avalanche.

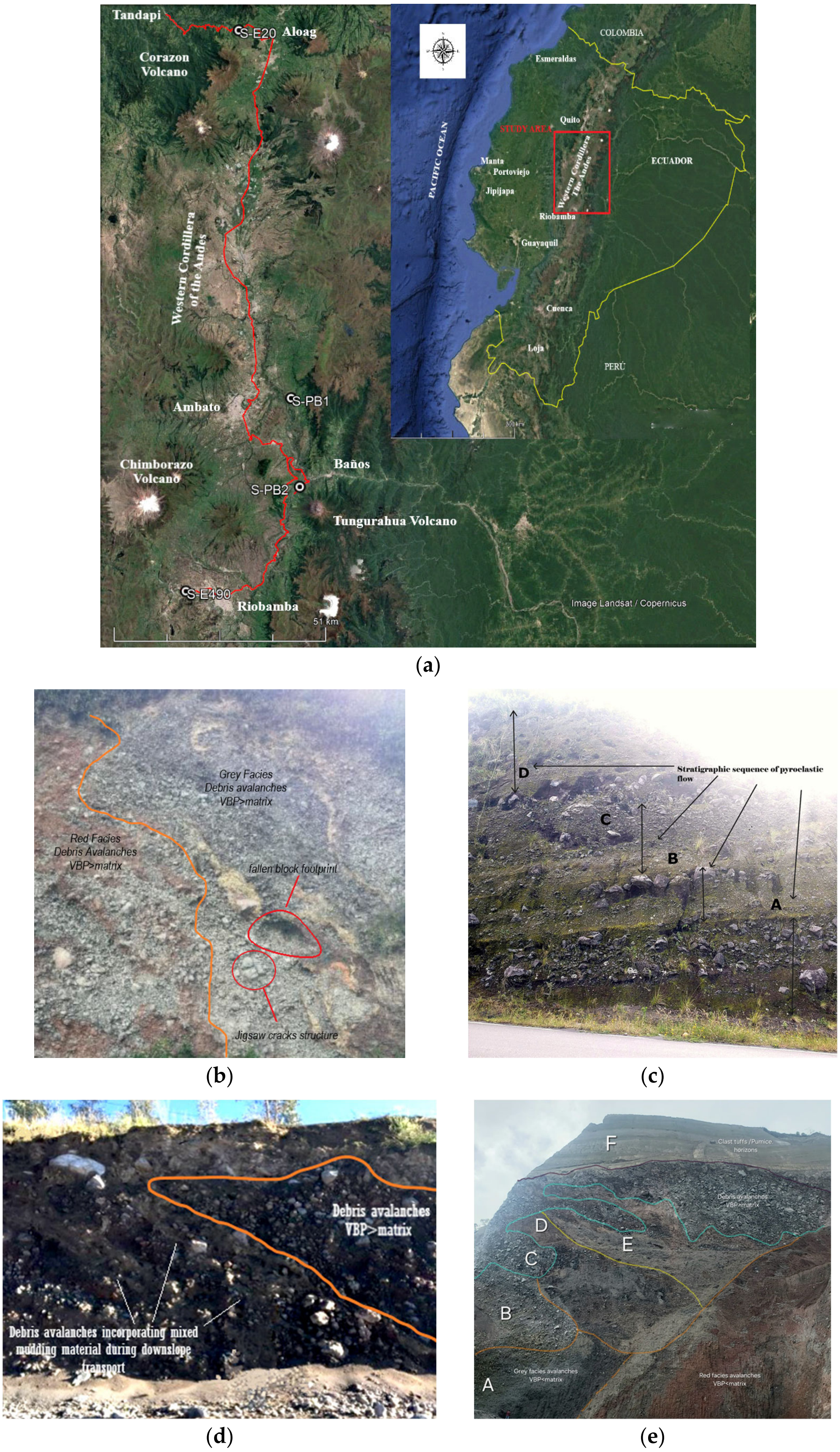


**Figure 6.** Road slopes in the Western Cordillera of Ecuador where the geomechanical characterization proposed is applied: (**a**) General location of the four slopes. (**b**) Slope S-PB1. (**c**) Slope S-PB, A, B, C, and D refers to four pyroclastic flow events identified; (**d**) Slope S-E490. (**e**) Slope S-E20, from the five levels identified (A to F); levels B and C correspond to bimrock materials.

At slope S-PB2, with a total height of 35 m, four pyroclastic flow events were identified, observed in decreasing grain size: blocks, gravel, sand, and fine particles. Interlocking of the blocks was also observed, following the dip of the slope and showing the direction in which the flow moved. Materials of this slope were classified as pyroclastic flows. From the four bimrock levels identified only one was studied, the one corresponding to the base of the slope, as this level was considered in the field the one that most affects the slope stability.

At slope S-E490, with a total height of 8 m, between 7 and 8 m thick rocks, with a coloration that varies from cream to reddish were observed; they were formed by different volcanic facies (Aphanitic, Vesicular, Phaneritic) in the same volcanic event, differentiated by their coloration and their mineral content. Jigsaw cracks were also observed in the deposit. The clast diameter was heterogeneous, its matrix presenting sizes ranging from 16 cm to 0.5 cm, and varying laterally to a finer matrix that encompasses the blocks. All in all, this slope was classified as a debris avalanche.

Finally, slope S-E20 had a total height of 47 m and consisted of andesite clasts with a silty sand matrix. Heterometric blocks of more than 1 m in diameter were observed. The blocks had gray to brown colors, a product of alteration and iron oxides. The matrix had clasts whose sizes varied from 0.1 cm to approximately 16 cm. The base of the outcrop had gray clasts in a humid granular matrix. Different events were observed that indicate its Quaternary history with different epiclastic deposits, products of its transport on the top of a sequence of ash with fall material with pumice horizons. This slope was also classified as a debris avalanche, and, from the different materials found, 17 m were considered bimrocks affecting the slope stability (see Figure 6e).

Three studied slopes were therefore classified as debris avalanche, and one slope as pyroclastic flow. In all cases, the parameter block size range was found between decimetric to metric values. Slopes S-PB1 and S-E20 showed similar block size ranges (from 0.85 m to 12.75 m), being the corresponding boundaries larger than the ones of the other two slopes. Slope S-PB2, identified as a pyroclastic flow, exhibited the lowest block size range boundaries.

In terms of the VBP, higher percentages of blocks of rock were found in debris avalanche deposits compared to the pyroclastic flow deposit. The VBP at slopes S-E20 and S-PB1 was equal or greater than 75%, indicating that these debris avalanche deposits are expected [7] to exhibit higher strength and, therefore, greater stability. This explains how a slope of high height (47 m and 17 m for slopes S-E20 and S-PB1, respectively) can withstand slopes angles of 70°. The VBP for slope S-E490, also a debris avalanche deposit, was slightly lower (55%); in this case, the slope angle was also 70°, but slope height was much lower, only 8 m. This is reasonable with the lower values of VBP, which should translate into lower strength and stability; however, an analysis of the matrix strength (which is addressed below) will help gain a better understanding of the stability.

Slope S-PB2 shows a low VBP, consistent with its pyroclastic flow nature. Although the VBP is low, the inclination of this slope attains 65°, with a total slope height of 35 m. This can be explained due to the natural sandy cement found in these materials as well as the presence of thin layers of ignimbrites in the whole slope; however, this pyroclastic flow bimrock can easily suffer erosion since the cement may be washed down by water, so its stability is a bit precarious.

Rock blocks characterization shows that the blocks of rock UCS at debris avalanches slopes S-E20 and S-PB1 are around 90 MPa, while, at the slope S-E490 this value is 45 MPa; this may indicate a higher weathering grade. UCS at pyroclastic flow slope S-PB2 yields a similar value, 57 MPa; thus, being the weathering grade is alike. Block friction angles are found about 30° in the three debris avalanches slopes, while such angle increases to 44° in the pyroclastic flow slope, due to the angular nature of the blocks.

Table 4 displays the XRF analysis conducted on matrix samples taken from the S-E490 slope, together with those found in the literature for previous studies [55] from areas near the Corazón Volcano. Both results show a good agreement. The total alkali ($Na_2O$ + $K_2O$) and silica ($SiO_2$) contents, plotted on a TAS diagram (Figure 7), suggest that the matrix consists of andesite and basaltic andesite origin. It should be noted that blocks of rock at this slope were also identified as andesite in nature, suggesting andesite as the parent rock of both blocks and the matrix.

**Table 4.** Chemical compounds (main oxides) obtained in the XRF analysis conducted at matrix samples taken from the S-E490 slope.

| Chemical Compound | Samples Taken at S-E490 | | Santamaría et al. [55] Results [1] | | | |
|---|---|---|---|---|---|---|
| $SiO_2$ | 59.30 | 54.30 | 62.28 | 54.84 | 58.97 | 57.56 |
| FeO | 7.64 | 7.49 | 6.06 | 8.63 | 7.42 | 7.71 |
| $Al_2O_3$ | 16.50 | 15.80 | 16.27 | 16.79 | 17.53 | 17.30 |
| $C_aO$ | 2.15 | 1.12 | 5.48 | 8.15 | 6.57 | 6.74 |
| MgO | 1.50 | 1.10 | 2.62 | 5.63 | 3.15 | 3.93 |
| $Na_2O$ | 3.30 | 4.35 | 3.96 | 3.81 | 4.18 | 4.27 |
| $K_2O$ | 1.04 | 0.97 | 1.48 | 0.97 | 1.17 | 1.25 |

[1] For the sake of the brevity, only 4 samples are shown.

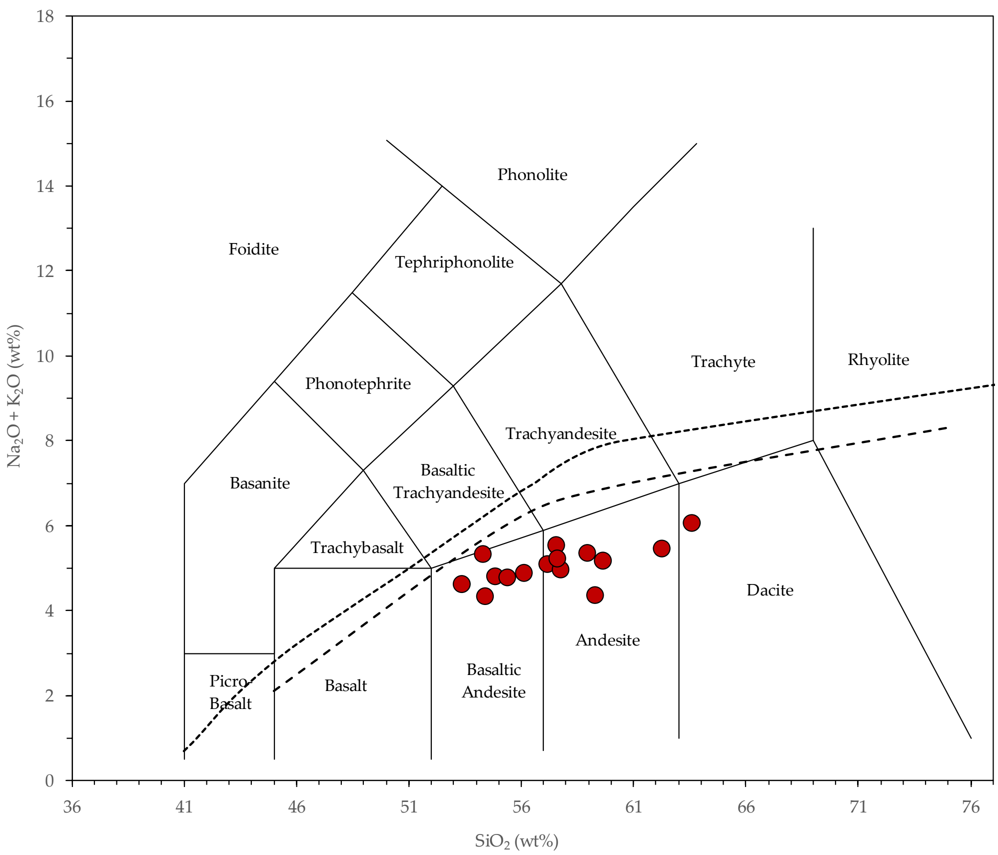


**Figure 7.** TAS diagram for genetic classification of the volcanic matrix of S-E20 slope from the chemical compounds obtained in the XRF analyses (Table 4).

Results of XRD analysis (Figure 8) indicate the spectral presence of labradorite, diopside and cristobalite as major constituents. This suggests that the fines in the bimrock matrix contain approximately 11% of clay minerals.

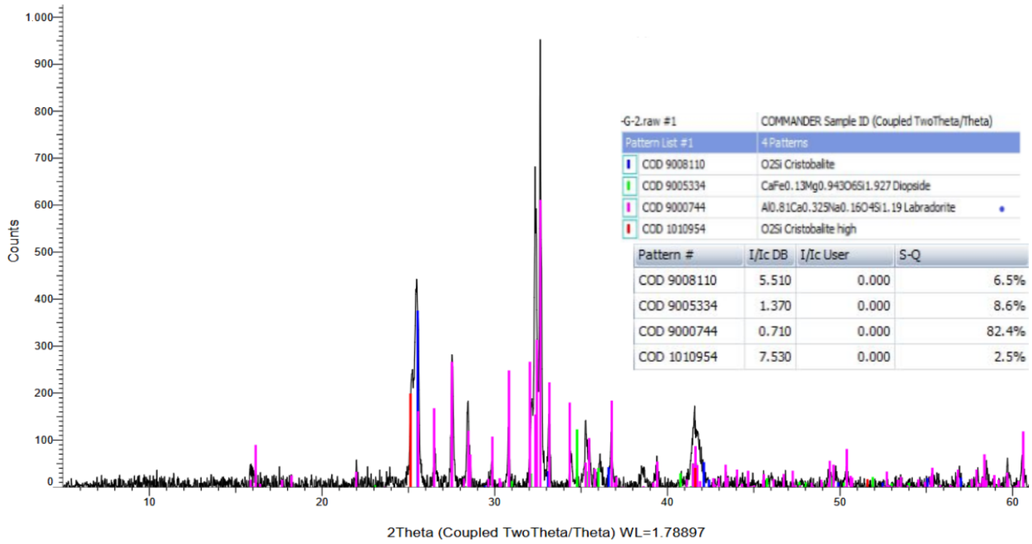


**Figure 8.** XRD analysis conducted at matrix samples taken from S-E20 slope.

Figure 9 presents the matrix gradation curve for that slope (24.42% gravel, 68.05% sand, and 10.50% fines). A uniformity coefficient larger than 6 suggests that the bimrock matrix exhibits a certain degree of particle size diversity, resulting in a good strength and stability of the matrix; however, a coefficient of curvature lower than 1 suggests the potential presence of voids or gaps between particles. Thus, the matrix exhibits poor sorting of its granular components, which may lead to low consistency and susceptibility to deformation and failure, thus affecting slope stability. In terms of plasticity, Atterberg's Plastic Limit [46] could not be performed, proving the silty nature of the matrix fines, already evidenced by the XRD analysis (where only 11% were clay minerals). According to the USCS [47], the matrix was classified as SP-SM, indicating high permeability and low moisture retention.

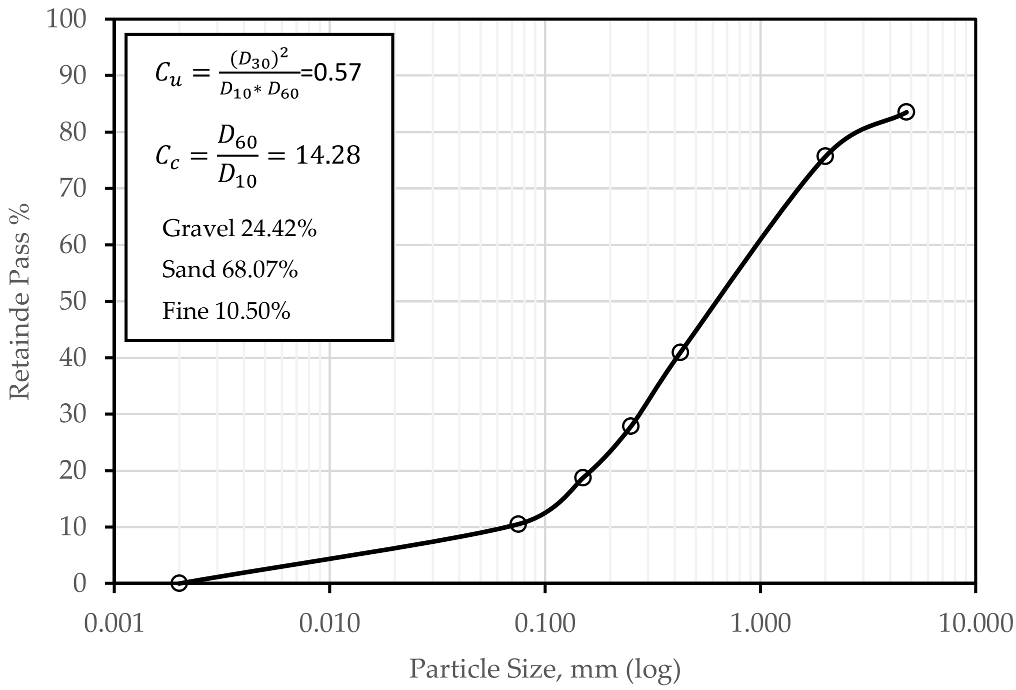


**Figure 9.** Gradation curve for a matrix sample taken at S-E490 slope.

All in all, grain size distribution shows that the bimrock is composed mainly of granular materials, with a lower proportion of clayey fines. That provides insight into the failure behavior of the bimrock matrix that encloses the blocks. Deformation is suggested to be primarily governed by the friction angle of the granular materials, which are themselves derived from the parent rock source.

Matrix strength parameters were only obtained at the S-E490 slope, because it was not possible to take undisturbed samples at the other three locations. This evidences the challenge of having high-quality samples in volcanic deposits of the Western Cordillera of Ecuador. The direct shear test results conducted on the bimrock matrix (following ASTM D3080 [48] and testing three specimens) are given in Figure 10. Horizontal displacement vs. shear stress curves (Figure 10a) reveal an initial elastic phase, extending to 0.5 mm of horizontal displacement in all specimens. Afterwards, an internal particle rearrangement within the matrix material occurs, until reaching a horizontal displacement of about 1.5 mm. Beyond that, the matrix continues to gain strength, and finally the stress-displacement curve shows an asymptotically horizontal trend.

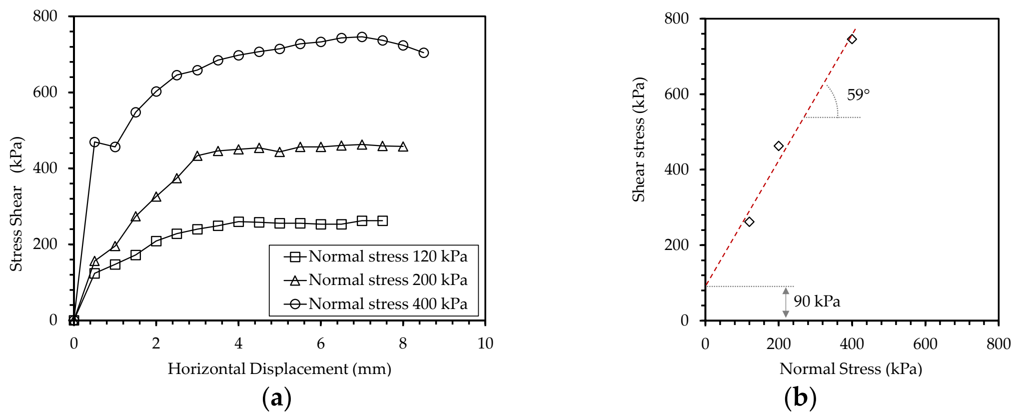


**Figure 10.** Direct shear test results of the bimrock matrix at S-E490 slope: (**a**) Horizontal displacement vs. shear stress curves; (**b**) Mohr-Coulomb failure envelope.

The Mohr–Coulomb failure envelope (Figure 10b) shows the shear strength parameters obtained, a cohesion equal to 90 kPa and a friction angle equal to 59°. These values are similar to those reported in the literature [10] for unwelded bimrock matrix materials. In addition, the high friction angle obtained (with a significant value of cohesion) also explains why this bimrock material (slope S-E490), where the 45% of the material corresponds to the matrix, can withstand a slope of 8 m with an angle of 70°.

## 4. Analysis and Discussion

The application of the proposed geomechanical characterization to four road slopes at the Western Cordillera of Ecuador has shown its ability to define a framework for systematically investigating any unwelded volcanic bimrock, gathering the most important data for the outcrop, and conducting the most convenient in situ and laboratory tests to characterize the volcanic bimrock. It considers the criteria of geotechnical significance already stated in the literature for bimrocks (e.g., [2,5,6,11,20]), common geotechnical parameters (like rock UCS), and the classification of the volcanic deposit in three types (debris avalanche, pyroclastic flow, or lahar), with this classification a novelty of this proposal. Establishing whether the deposit corresponds to an initiation phase or a transport phase of volcanic activity [40] helps in understanding their engineering performance as a slope.

The proposed geomechanical characterization is therefore a first step to assess the potential stability of unwelded volcanic bimrock slopes. The parameters obtained through the application of the geomechanical characterization provide an insight into the expected mechanical behavior, strength, and deformation, not only in terms of the blocks of rock and the matrix, but also of the bimrock material as a whole For instance, the presence of a wide block size range and matrix gradation, combined with appropriate water content, is expected to enhance interparticle bonding, thereby increasing resistance to failure. Moreover, a medium-high VBP (above 60%) may indicate good mechanical behavior, able to withstand steep and/or high slopes, increasing this performance for rising values of the VBP. This fact was seen in the three debris avalanches slopes assessed in this work (S-PB1, S-E490, and S-E20 slopes), and it aligns with the conceptual relationship between the internal friction angle of bimrocks and VBP already established in the literature [5–8,10].

Conversely, a low VBP (slightly above 25%) is normally bound to having high fine content and an expected poor mechanical behavior. This can be attributed to the weak bonding between the blocks of rock and the matrix, leading to limited block interlocking. Typically, debris avalanche deposits will be expected to have medium to high VBP compared to pyroclastic flows and lahars. Thus, having an idea of the volcanic deposit types provides worthy preliminary information. That may also be a key aspect, as was demonstrated at slope S-PB2: even with a low VBP, the slope is able to withstand a slope of 65° with a significant height (35 m), likely because of the nature of the deposit. Thus, the sandy matrix with some cementing properties and the existence of hard layers (ignimbrites in this case), are features associated with a pyroclastic flow.

In addition, studying the geological characteristics of the volcanic deposit can provide further interesting information. Thus, a higher degree of interlocking due to inclined or embedded blocks within the matrix may contribute to having greater strength, whereas horizontal or elliptical block orientations may reduce the strength and stability of bimrocks. This argument might be important when a low VBP, orientation and shape of rock blocks within the matrix have an influence on the bimrock behavior in such cases [6]. Other works can be found in the literature regarding the effect of block shape and orientation on the strength of bimrocks [16].

Visual lithological identification of rock blocks and matrix XRF analyses allow us to determine if blocks and matrix components are of different origins, while XRD analyses allow for identifying a high percentage of clay minerals with potential problematic issues. Together with the gradation curve, they show if the matrix strength is mostly dominated by the internal friction angle of particles, or if a significant cohesion is expected (probably, associated with lower friction angles). In cases where the matrix is essentially granular, with absence or very low content of clayey fines, and the VBP is medium-high, one may consider the whole bimrock behaves as a granular material, with its friction angle controlled by the relative density. However, further research is needed to support this hypothesis.

Chemical compounds obtained by XRF also provide an insight into the behavior of the bimrock deposit against weathering. This may be especially important in tropical and mid-mountain regions, as is the case in the studied area. Table 4 shows a high amount of silica ($SiO_2$), which is normally associated with a good mechanical stability. However, the presence of significant quantities of aluminum and iron oxides ($Al_2O_3$ and FeO) may represent weakness factors under certain environmental conditions. Thus, chemical compounds may be relevant to understand the geomechanical performance of unwelded volcanic bimrocks and its susceptibility to weathering and alteration in highly rainy regions.

Some studies conducted on bimrocks, both welded and unwelded [8–10,13,14,16,19], state that the mechanical behavior of these materials and their overall strength and stiffness depend mainly on the contrast in resistance between blocks of rock and matrix. In addition, some studies have tried to establish the strength parameters of a bimrock as a whole, following Mohr–Coulomb or Hoek–Brown failure criteria, from the individual values of strength parameters of the blocks of rock and the matrix, such as the matrix friction angle, the matrix cohesion, and the rock blocks UCS [6,8,10,13,58,59]. Since those parameters are gathered when following the proposed geomechanical characterization, this may be considered a first step for designing slopes on unwelded volcanic bimrock materials as well as designing stabilization measures at slopes where such materials are present. However, it is important that the geomechanical characterization of a bimrock does not strongly depend on sampling and laboratory testing, since both procedures are challenging in bimrocks. This aspect, already stated in the literature [20,25], was experienced in three of the four Ecuadorian slopes analyzed.

All in all, the geomechanical characterization proposed is expected to reduce the uncertainty of constructions dealing with unwelded volcanic bimrock, as well as to support the decision-making process regarding the need for appropriate stabilization measures on slopes with this type of heterogeneous material. This methodology also represents an advancement in sustainable construction practices and landslide risk mitigation in hazardous areas like Ecuador and other Andean countries. Not for nothing, Ecuadorian government initiatives like the “Plan Nacional para el Buen Vivir 2017–2021” [30,60] promote a sustainable development while addressing the impact of landslides on its territory, focusing on resilience and risk reduction. Moreover, the climate change is especially intense in areas like Ecuador and other countries of the Andean Cordillera [61], regions where volcanic bimrocks materials are very common; all of which demands a fast adaptation by the scientific community and social stakeholders towards a potential increase in landslides events in the Andean region.

## 5. Conclusions

This paper has presented a geomechanical characterization for unwelded volcanic bimrock materials, oriented towards their performance in terms of slope stability and landslide hazard occurrence. The characterization includes assessing both the geological and geotechnical features of unwelded volcanic bimrock deposits. It classifies the deposits into three types (debris avalanche, pyroclastic flow, and lahar), analyzes the rock blocks and matrix geotechnical properties, as well as their composition, and defines indices like the block size range and the VBP that characterize each slope. These aspects provide a reliable framework to estimate the expected behavior and its stability. It is also a first and fundamental step before addressing by common modeling tools the design of the slope and/or the stabilization measures needed.

The geomechanical characterization proposed was applied to four volcanic bimrock slopes belonging to the Western Cordillera of Ecuador. The heterogeneity of these materials has generated a wide uncertainty in the engineering practices, with multiple landslides associated with such materials having been recorded in recent years. The geomechanical characterization proposed showed to be capable of capturing the main geological and geotechnical engineering features that define each slope, and the analysis of the different parameters and indices obtained provides a reliable framework for explaining the actual stability of the slopes. The systematic approach proposed here may thus result in a keystone of sustainable construction practices towards landslide risk mitigation in the Andean countries and other regions where unwelded volcanic bimrocks are present.

Some further work is nonetheless needed in terms of understanding the mechanical behavior of unwelded volcanic bimrocks. The effect on the bimrock resistance and strength of the rock block shape and their orientation with respect to the orientation of the slope is not clear, and, even though the geomechanical characterization incudes a description of the deposit, these issues are not directly considered. Similarly, hydrogeological aspects are not directly considered in the characterization, not are the effects of seismic activity or erosional processes. Should some of these parameters become important, such information must be included in the bimrock characterization.

**Author Contributions:** Conceptualization, M.P.-Z., J.G.-R. and F.J.T.; methodology, M.P.-Z. and J.G.-R.; validation, J.G.-R., F.J.T. and O.A.-P.; formal analysis, J.G.-R., F.J.T. and O.A.-P.; investigation, M.P.-Z., J.G.-R. and F.J.T.; resources, M.P.-Z. and O.A.-P.; data curation, M.P.-Z.; writing—original draft preparation, M.P.-Z. and O.A.-P.; writing—review and editing, J.G.-R., F.J.T. and O.A.-P.; visualization, M.P.-Z. and J.G.-R.; supervision, J.G.-R. and F.J.T. All authors have read and agreed to the published version of the manuscript.

**Funding:** Funded with Aid for First Research Projects (PAID-06-24), Vice-rectorate for Research of the Universitat Politècnica de València (UPV).

**Institutional Review Board Statement:** Not applicable.

**Informed Consent Statement:** Not applicable.

**Data Availability Statement:** The data is available upon request.

**Acknowledgments:** The first author thanks the Universidad Central del Ecuador for the scholarship provided to conduct a stay in Spain during his PhD Studies. Thanks are also given to A. Llumigusin and F. Tarco, students of the Geotechnics subject, and J. Bustillos, a teacher of Geology at Universidad Central del Ecuador, for their collaboration in data gathered in the field.

**Conflicts of Interest:** The authors declare no conflicts of interest.

## References

1. Raymond, L.A. *Classification of Melanges, Melanges: Their Nature, Origin, and Significance*, 1st ed.; The Geological Society of America, Inc.: Boulder, CO, USA, 1984.
2. Medley, E. The Engineering Charaterization of Melanges and Similar Block in Matriz (Bimrocks). Ph.D. Thesis, University of California at Berkeley, Berkeley, CA, USA, 17 July 1994.
3. Morales Romero, S.O. Methodological Guidelines for the Characterization of Mixtures Materials Soil-Rock Bimsoils Type. Master's Thesis, Complutense University of Madrid, Madrid, Spain, 10 July 2022.
4. Medley, E.; Sanz, P. Characterization of Bimrocks (Rock/Soil Mixtures) with Application to Slope Stability Problems. In Proceedings of the Eurock 2004 and the 53rd Geomechanics Colloquium, Salzburg, Austria, 7–9 October 2004.
5. Lindquist, E.S.; Medley, E. The engineering significance of the scale-independence of some Franciscan melanges in California, USA. In Proceedings of the 35th U.S Symposium on Rock Mechanics, USRMS, Reno, NV, USA, 5–7 June 1995.
6. Lindquist, E.S.; Goodman, R.E. Strength and deformation properties of a physical model melange. In Proceedings of the 1st North American Rock Mechanics Symposium, Austin, TX, USA, 1–3 June 1994.
7. Medley, D.; Zekkos, D. Geopractitioner approaches to working with antisocial mélanges. In *Mélanges: Processes of Formation and Societal Significance*; Wakabayashi, J., Dilek, Y., Eds.; The Geological Society of America: Boulder, CO, USA, 2011.
8. Sonmez, H.; Kasapoglu, K.E.; Coskun, A.; Tunusluoglu, C.; Medley, E.W.; Zimmerman, R.W. A Conceptual empirical approach for the overall strength of unwelded. In Proceedings of the ISRM Regional Symposium Eurock, Dubrovnik, Croatia, 29–31 October 2009.
9. Sonmez, H.; Tuncay, C.; Gokceoglu, C. Models to predict the uniaxial compressive strength and the modulus of elasticity for Ankara Agglomerate. *J. Rock Mech. Mining Sci.* **2004**, *41*, 717–729. [CrossRef]
10. Kalender, A.; Sonmez, H.; Medley, E.; Tunusluoglu, C.; Kasapoglu, K.E. An approach to predicting the overall strengths of unwelded bimrocks and bimsoils. *Eng. Geol.* **2014**, *183*, 65–79. [CrossRef]
11. Wen-Jie, X.; Qiang, X.; Rui-Lin, H. Study on the shear strength of soil–rock mixture by large scale direct shear test. *Int. J. Rock Mech. Min. Sci.* **2011**, *48*, 1235–1247. [CrossRef]

12. Sonmez, H.; Gokceoglu, C.; Medley, E.W.; Tuncay, E.; Nefeslioglu, H.A. Estimating the uniaxial compressive strength of a volcanic bimrock. *Int. J. Rock Mech. Min. Sci.* **2006**, *43*, 554–561. [CrossRef]
13. Sonmez, H.; Altinsoy, H.; Gokceoglu, C.; Medley, E.W. Considerations in developing an empirical strength criterion for bimrocks. In Proceedings of the 4th Asian Rock Mechanics Symposium (ARMS 2006), Singapore, 6–10 November 2006.
14. Coli, M.; Berry, P.; Boldini, D. In situ non-conventional shear tests for the mechanical characterisation of a bimrock. *Int. J. Rock Mech. Min. Sci* **2011**, *48*, 95–102. [CrossRef]
15. Kahraman, S.; Alber, M. Estimating unconfined compressive strength and elastic modulus of a fault breccia mixture of weak blocks and strong matrix. *Int. J. Rock Mech. Min. Sci.* **2006**, *43*, 1277–1287. [CrossRef]
16. Jiménez-Rodríguez, R. *Ingeniería de Rocas. Caracterización de Macizos Rocosos y Teoría de Bloques para Estabilidad de Taludes: Un Enfoque Probabilístico*, 1st ed.; Ibergarceta Publicaciones, S.L.: Madrid, Spain, 2015.
17. Goodman, R.E.; Shi, G.-h. *Block Theory and Its Application to Rock Engineering*; Prentice-Hall: Englewood Cliffs, CA, USA, 1985.
18. Hudson, J.A.; Priest, S.D. Discontinuities and rock mass geometry. *Int. J. Rock Mech. Min. Sci.* **1979**, *16*, 339–362. [CrossRef]
19. Sonmez, H.; Ercanoglu, M.; Kalender, A.; Dagdelenler, G.; Tunusluoglu, C. Predicting uniaxial compressive strength and deformation modulus of volcanic bimrock considering engineering dimension. *Int. J. Rock Mech. Min. Sci* **2016**, *86*, 91–103. [CrossRef]
20. Nikolaidis, G.; Saroglou, C. Engineering geological characterisation of block-in-matrix rocks. *BGSG Bull. Geol. Soc. Greece* **2016**, *50*, 874–884. [CrossRef]
21. Wang, S.; Zhu, Y.; Ma, W.; Wang, Z.; Li, G. Effects of rock block content and confining pressure on dynamic characteristics of soil-rock mixtures. *Eng. Geol.* **2021**, *280*, 105963. [CrossRef]
22. Napoli, M.L.; Barbero, M.; Ravera, E.; Scavia, C. A stochastic approach to slope stability analysis in bimrocks. *Int. J. Rock Mech. Min. Sci.* **2018**, *1*, 41–49. [CrossRef]
23. Napoli, M.L.; Barbero, M.; Scavia, C. Effects of block shape and inclination on the stability of melange bimrocks. *Bull. Eng. Geol. Environ.* **2021**, *80*, 7457–7466. [CrossRef]
24. Napoli, M.L.; Barbero, M.; Scavia, C. Tunneling in heterogeneous rock masses with a block-in-matrix fabric. *Int. J. Rock Mech. Min. Sci.* **2021**, *138*, 1365–1609. [CrossRef]
25. Afifipour, M.; Moarefvand, P. Mechanical behavior of bimrocks having high rock block proportion. *Int. J. Rock Mech. Min. Sci.* **2014**, *65*, 40–48. [CrossRef]
26. Alonso-Pandavenes, O.; Torres, G.; Torrijo, F.J.; Garzón-Roca, J. Basement tectonic structure and sediment thickness of a valley defined using HVSR geophysical investigation, Azuela valley, Ecuador. *Bull. Eng. Geol. Environ.* **2022**, *81*, 210. [CrossRef]
27. Alonso-Pandavenes, O.; Torrijo, F.J.; Garzón-Roca, J.; Gracia, A. Early Investigation of a Landslide Sliding Surface by HVSR and VES Geophysical Techniques Combined, a Case Study in Guarumales (Ecuador). *Appl. Sci.* **2023**, *13*, 1023. [CrossRef]
28. Alonso-Pandavenes, O.; Bernal, D.; Torrijo, F.J.; Garzón-Roca, J. A Comparative Analysis for Defining the Sliding Surface and Internal Structure in an Active Landslide Using the HVSR Passive Geophysical Technique in Pujilí (Cotopaxi), Ecuador. *Land* **2023**, *12*, 921. [CrossRef]
29. Torrijo, F.J.; Álvarez, S.; Garzón-Roca, J. A Case Study of a Macro-Landslide in the High Mountain Areas of the Ecuadorian Andes: "La Cría" at the Azuay Province (Ecuador). *Land* **2024**, *13*, 2047. [CrossRef]
30. Alonso-Pandavenes, O.; Torrijo, F.J.; Garzón-Roca, J. Sustainable management of landslides in Ecuador: Leveraging geophysical surveys for effective risk reduction. *Sustainability* **2024**, *16*, 10797. [CrossRef]
31. Ponce-Zambrano, M.R.; Ibadango, C.E.; Merino, J.; Cervantes, H.; Ortiz, J. Application of support methodologies in low shear strength materials on the Calacali-Nanegalito route. In Proceedings of the 1st Chilean Conference of Rock Mechanics, Santiago de, Chile, Chile, 22–24 November 2023.
32. Flentje, P.; Chowdhury, R. Resilience and Sustainability in the Management of Landslides. *Proc. Inst. Civ. Eng.—Eng. Sustain.* **2018**, *171*, 3–14. [CrossRef]
33. Cobos, G.; Eguibar, M.A.; Torrijo, F.J.; Garzón-Roca, J. A Case Study of a Large Unstable Mass Stabilization: "El Portalet" Pass at the Central Spanish Pyrenees. *Appl. Sci.* **2021**, *11*, 7176. [CrossRef]
34. Azadi, H.; Petrescu, D.C.; Petrescu-Mag, R.M.; Ozunu, A. Special Issue: Environmental Risk Mitigation for Sustainable Land Use Development. *Land Use Policy* **2020**, *95*, 104488. [CrossRef]
35. Mineo, S.; Pappalardo, G.; Mangiameli, M.; Campolo, S.; Mussumeci, G. Rockfall Analysis for Preliminary Hazard Assessment of the Cliff of Taormina Saracen Castle (Sicily). *Sustainability* **2018**, *10*, 417. [CrossRef]
36. Mineo, S.; Pappalardo, G. Sustainable Fruition of Cultural Heritage in Areas Affected by Rockfalls. *Sustainability* **2020**, *12*, 296. [CrossRef]
37. Mineo, S.; Pappalardo, G.; Onorato, S. Geomechanical Characterization of a Rock Cliff Hosting a Cultural Heritage through Ground and UAV Rock Mass Surveys for Its Sustainable Fruition. *Sustainability* **2021**, *12*, 924. [CrossRef]
38. *ASTM D2488*; Standard Practice for Description and Identification of Soils (Visual-Manual Procedures). American Society of Testing Materials: West Conshohocken, PA, USA, 2018.

39. Murcia, M.F.; Borrero, C.A.; Pardo, N.; Alvarado, G.A.; Arnosio, M.; Scolamacchia, T. Volcaniclastic deposits: Terminology and concepts for a classification in Spanish. *Rev. Geol. Am. Cent.* **2013**, *48*, 15–39.
40. Bernard, B.; Takarada, S., S.; Andrade, D.; Dufresne, A. Terminology and Strategy to Describe Large Volcanic Landslides and Debris Avalanches. In *Volcanic Debris Avalanches*; Matteo Roverato, A., Dufresne, J.P., Eds.; Springer: Cham, Switzerland, 2021.
41. Etinger, S.; Mothes, P.; Paris, P.; Schilling, S. The 1877 lahar deposits on the eastern flank of Cotopaxi volcano. *Géomorphologie Relief Process. Environ.* **2007**, *13*, 271–280. [CrossRef]
42. Ulusay, R. *The ISRM Suggested Methods for Rock Characterization, Testing and Monitoring: 2007–2014*; Springer: Cham, Switzerland, 2015.
43. *ASTM D7263*; Standard Test Methods for Laboratory Determination of Density and Unit Weight of Soil Specimens. American Society of Testing Materials: West Conshohocken, PA, USA, 2021.
44. *ASTM D1556*; Standard Test Method for Density and Unit Weight of Soil in Place by Sand-Cone Method. American Society of Testing Materials: West Conshohocken, PA, USA, 2024.
45. *ASTM D2216*; Standard Test Method for Laboratory Determination of Water (Moisture) Content of Soil and Rock by Mass. American Society of Testing Materials: West Conshohocken, PA, USA, 2017.
46. *ASTM D422*; Standard Test Method for Particle-Size Analysis of Soils. American Society of Testing Materials: West Conshohocken, PA, USA, 2014.
47. *ASTM D4318*; Standard Test Methods for Liquid Limit, Plastic Limit, and Plasticity Index of Soils. American Society of Testing Materials: West Conshohocken, PA, USA, 2018.
48. *ASTM D2487*; Standard Practice for Classification of Soils for Engineering Purposes (Unified Soil Classification System). American Society of Testing Materials: West Conshohocken, PA, USA, 2020.
49. *ASTM D3080*; Standard Test Method for Direct Shear Test of Soils Under Consolidated Drained Conditions. American Society of Testing Materials: West Conshohocken, PA, USA, 2012.
50. *ASTM D4767*; Standard Test Method for Consolidated Undrained Triaxial Compression Test for Cohesive Soils. American Society of Testing Materials: West Conshohocken, PA, USA, 2020.
51. Aristizábal, E.; Riaño, F.; Jiménez-Ortiz, J. Rainfall thresholds as triggering factor in the Central cordillera of the Colombian Andes. *Bol. Geol.* **2022**, *44*, 183–197. [CrossRef]
52. Pichincha Provincial Government, GPP. *Developement and Management Territorial Plan of Manuel Cornejo Astorga–TANDAPI 2012–2025*; GPP: Quito, Ecuador, 2012.
53. Vallejo, C. Evolution of the Western Cordillera in the Andes of Ecuador (Late Cretaceous-Paleogene). PhD. Thesis, Eidgenössische Technische Hochschule ETH Zürich, Zurich, Switzerland, 2007.
54. Hidalgo, S. Interacciones Entre Magmas Clásicas" y Adriáticas Calco-Alcalinali: Ejemplo del Complejo Volcánico Atacazo-Ninahuilca (Ecuador). PhD. Thesis, Université Blaise Pascal, Clermond, France, 2006.
55. Santamaria, S.; Quidelleur, J.; Samaniego, P.; Audin, L.; Le Pennec, J. Timing of Quaternary volcanism and its relationship with tectonics in the central segment of the Ecuadorian Andes. *J. Volcanol. Geotherm. Res.* **2023**, *442*, 107895. [CrossRef]
56. National Direction of Geology and Mining. *National Geological Chart of Ecuador 1:100.000, Machachi Sheet*; National Direction of Geology and Mining of Ecuador: Quito, Ecuador, 1978.
57. Benjamin, B.; Andrade, D. *Quaternary Volcanos in Continetal Ecuador*; Institud de Recherche pour le Développement IRD: Marselle, France, 2016.
58. Lindquist, E.S. The Strength and Deformation Properties of Mélange. Ph.D. Dissertation, Univesity of California at Berkeley, Berkeley, CA, USA, 1994.
59. Nanclares, F.J. Mechanical Behavior of Granular Soils of Alluvial Origin. Ph.D. Dissertation, National Unversity of Colombia, Bogotá, Colombia, 2018.
60. SENPLADES Plan Nacional para el Buen Vivir 2017–2021. 2017. Available online: https://www.gobiernoelectronico.gob.ec/wp-content/uploads/downloads/2017/09/Plan-Nacional-para-el-Buen-Vivir-2017-2021.pdf (accessed on 22 September 2024).
61. Puente-Sotomayor, F.; Egas, A.; Teller, J. Land Policies for Landslide Risk Reduction in Andean Cities. *Habitat Int.* **2021**, *107*, 102298. [CrossRef]